2011 International Conference on Computer and Automation Engineering (ICCAE 2011)
IPCSIT vol. 44 (2012) © (2012) IACSIT Press, Singapore
DOI: 10.7763/IPCSIT.2012.V44.4

Comparisons of Two Detectors for a Tradeoff between Complexity and Performance in MIMO-OFDM Systems

Jin Ren[a +] and Seokhyun Yoon[b]

Department of Electronics Engineering
Dankook University, Yongin-si, Gyeonggi-do, Korea

Abstract. Recent works on detector algorithms in multiple-input multiple-output orthogonal frequency division multiplexing (MIMO-OFDM) system were mainly focused on sphere detector, which provides a tradeoff between complexity and performance by suitably choosing the “radius” or the number of candidates in the search space. Meanwhile, another approach, called poly-diagonalization and trellis detector, has been proposed to compromise the complexity and performance in [13] and developed in [14]. In this paper, we compare sphere decoding and asymmetrical poly-diagonalization approach with the variable in terms of both complexity and performance. The performance is evaluated in frequency selective fading channel environment on the basis of orthogonal frequency division multiplexing with channel codes, where the generation of soft decision values is crucial. The results show that the performances of poly-diagonalization approach and sphere decoding have their own advantages at low and high computational complexity respectively.

Keywords: coded mimo-ofdm; detector algorithms; frequency selective fading;

1. Introduction

The increasing data rates in wireless communication systems require large bandwidths. Orthogonal frequency division multiplexing (OFDM) [1] has become a widely used technique to significantly reduce receiver complexity in broadband systems. Multiple–input multiple-output (MIMO) channels offer improved capacity and significant potential for improved reliability compared to single antenna channels [2]. MIMO techniques in combination with OFDM (MIMO-OFDM) have been identified as a promising approach for high spectral efficiency wideband systems. A coded MIMO-OFDM system (i.e., with an outer channel coding) can obtain the diversity gain and the coding gain simultaneously, and hence, obtain additional performance improvement.

In order to take the full advantage of this capacity increase, efficient and reliable receivers need to be developed for successful application of such MIMO techniques. Traditionally, in the context of multiuser detection, the receivers are classified into three types, i.e., maximum likelihood (ML) detector [3], [4], linear detectors [5], [6], and Successive interference cancellation (SIC) detector [7]. Recently, however, other alternatives, such as the sphere decoding and the channel truncation approach, have been developed and studied rigorously. The Sphere detector (SD) [8-12] employs QR decomposition, which effectively triangularizes the channel and, utilizing this channel structure, it uses a sort of tree search, where, by reducing the search space, it can provide a tradeoff between the complexity and performance. It constitutes the most promising low complexity near-ML detector class, and hence its representatives have attracted substantial research attention. In general, the sphere decoding algorithm can be categorized into two types; depth-first search and breadth-first search algorithms. The *K*-best LSD algorithm (KLSD) in [9] is a breadth-first search algorithm having fixed complexity. More recently, a channel truncation approaches was proposed in [13] and [14]. Similar to the sphere decoding, it is also a two-stage detector where, in the first stage, it converts the

[+] Email: [a] renjin@dankook.ac.kr [b] wireless@dankook.ac.kr

channel into a poly-diagonal form and, by utilizing the poly-diagonal structure, it employs trellis search, rather than tree search. This scheme also can provide tradeoff between the complexity and performance by choosing an appropriate order of poly-diagonalization. In this paper, we compare *K*-best List Sphere detectors (KLSD) and Asymmetrical Poly-diagonalization and tail-biting trellis detectors (ASY-PD) with variable in coded transmissions and frequency selective fading channel environments. The generation of soft decision will also be included for performance and complexity comparison since it is crucial for the channel coding.

2. System Model

An OFDM-based MIMO transmission system is considered, with N_T transmit, N_R receive antennas and N_{sc} subcarriers, each of which employ a quadrature amplitude modulation (QAM) constellation of alphabet A of size $|A| = 2^{\Omega}$, where Ω denotes the number of bits per symbols. We denote the $N_T \times 1$ symbol vector for the kth subcarrier as

$$\mathbf{s}(k) = [s_1^t(k), \ldots, s_{N_T}^t(k)]^T \tag{1}$$

where $s_m^t(k)$ is the input symbol to the m-th transmit antenna on subcarrier k in the tth time, and $(\cdot)^T$ denotes the transpose operation. For each antenna, the number N_{sc} of data symbols are then passed to OFDM modulator, where the N_{sc} data symbols are transformed by inverse Discrete Fourier Transform (IDFT) and transmitted after adding the cyclic prefix (CP). The superscript t will be omitted in the sequel since it is clear from the context.

The received vector $\mathbf{y}(k)$ after removed CP and demodulated with Discrete Fourier Transform (DFT) and $\mathbf{n}(k)$ as a noise vector of length N_R can be expressed as

$$\mathbf{y}(k) = \mathbf{H}(k)\mathbf{s}(k) + \mathbf{n}(k),\ k = 0,\ \ldots,\ N_{sc} - 1 \tag{2}$$

where the DFT-transformed additive white Gaussian noise (AWGN) $\mathbf{n}(k)$ is assumed with zero mean and variance σ_n^2 per N_R receiver antenna with N_{sc} subcarriers.

The frequency MIMO channel impulse response can be described by N_{sc} complex channel matrices

$$\mathbf{H}(k) = \begin{bmatrix} \mathrm{H}_{1,1}(k) & \cdots & \mathrm{H}_{1,N_T}(k) \\ \vdots & \ddots & \vdots \\ \mathrm{H}_{N_R,1}(k) & \cdots & \mathrm{H}_{N_R,N_T}(k) \end{bmatrix},\ k = 0, \ldots, N_{sc} - 1 \tag{3}$$

of the dimension $N_R \times N_T$.

3. KLSD and ASY-PD

3.1. KLSD

This algorithm utilizes the so-called QR decomposition to convert the channel into a triangular form and, then, a sort of reduced tree search is used to determine the soft decision values. The QR decomposition can be performed either ZF sense or in MMSE sense. The QR decomposition in ZF sense is straightforward, i.e., we decompose the channel as $\mathbf{H} = \mathbf{QR}$ where $\mathbf{Q}$ is a unitary matrix and $\mathbf{R}$ is a triangular matrix. Hence, by multiplying $\mathbf{y}$ by $\mathbf{Q}^H$, the channel can be effectively converted into a triangular–type channel making it convenient for tree search. One of drawback in QR decomposition in ZF sense is the noise boost, as in ZF equalizer, especially for higher layer. And the QR decomposition in MMSE sense [9] would have better performance than that in ZF sense. As proposed in [9], it can be performed by the extended channel matrix, $\underline{\mathbf{H}}$, and the extended received vector, $\underline{\mathbf{y}}$, defined as

$$\underline{\mathbf{H}} = \begin{bmatrix} \mathbf{H} \\ \sigma_n \mathbf{I}_{N_T} \end{bmatrix} = \underline{\mathbf{Q}}\underline{\mathbf{R}} = \begin{bmatrix} \mathbf{Q}_1 \\ \mathbf{Q}_2 \end{bmatrix} \underline{\mathbf{R}} \text{ and } \underline{\mathbf{y}} = \begin{bmatrix} \mathbf{y} \\ \mathbf{0}_{N_T \times 1} \end{bmatrix} \tag{4}$$

where $\underline{\mathbf{Q}}$ is a $(N_T + N_R) \times N_T$ matrix with orthogonal column and $\underline{\mathbf{R}}$ is an $N_T \times N_T$ upper triangular matrix. By multiplying $\underline{\mathbf{y}}$ by $\underline{\mathbf{Q}}^H$, we have

$$\mathbf{y}' = \underline{\mathbf{Q}}^H \underline{\mathbf{y}} = \underline{\mathbf{R}}\mathbf{x} - \sigma_n \mathbf{Q}_2^H \mathbf{x} + \mathbf{Q}_1^H \mathbf{n} \tag{5}$$

where the second term in the right hand side is the residual interferences. The effective noise variance, $\sigma_{\hat{n},k}^2$, for the kth layer is given by the diagonal component of $\sigma_n^2(\underline{\mathbf{H}}^H\underline{\mathbf{H}})^{-1}$.

For the post-tree search algorithm, we consider the K-best LSD algorithm in [10] in this paper since its complexity is fixed. In the simulation, we use the same one in [10], which will be briefly described here. Let $\mathbf{s}_i^{N_T} = (s_i, s_{i+1}, \ldots, s_{N_T})^T$ denote a vector consisting of the last $N_T - i + 1$ elements of $\mathbf{s}$ and define the squared partial Euclidean distance (PED) at the ith layer as

$$d\left(\mathbf{s}_i^{N_T}\right) = \sum_{j=i}^{N_T} \frac{1}{\sigma_{\hat{n},j}^2} \left| y'_j - \sum_{l=j}^{N_T} r_{j,l} s_l \right|^2 \tag{6}$$

where $r_{j,l}$ is the (j,l)th element of the upper triangular matrix $\mathbf{R}$ or $\underline{\mathbf{R}}$. Note that we weighted the squared distance by the inverse of the effective noise variance. Based on the squared PED, the algorithm finds the fixed number K of symbols at each layer and stores them for the further tree search step. Once the algorithm finishes the tree search, the LLR for each bit, say mth, is given by

$$L_m = \min_{\mathbf{s}_i^{N_T} \in \Phi_m^1} d(\mathbf{s}_i^{N_T}) - \min_{\mathbf{s}_i^{N_T} \in \Phi_m^0} d(\mathbf{s}_i^{N_T}) \tag{7}$$

where $\Phi_m^b \subset A$ denotes the set of candidate symbol vectors (candidate list) whose mth bit is equal to b.

One problem in calculating (7) under the reduced K-best tree search is that LLR cannot be obtained when no surviving symbol candidates whose mth bit is either bit 0 or 1 remain. In [15-16], an efficient LLR clipping method to combat this problem was proposed in the following.

$$L_m^{clip} = \begin{cases} L_m & if\ |L_m| \le L_{\max} \\ \mathrm{sgn}(L_m) \cdot L_{\max} & if\ |L_m| > L_{\max} \end{cases} \tag{8}$$

The simulator takes into account the effect of LLR clipping with threshold $L_{\max} = 8$ [4].

3.2. ASY-PD

The detector is similar to the concatenated channel shortening equalizer and maximum likelihood sequence estimator, developed for Gaussian ISI channel. The poly-diagonalization can be regarded as a structured channel shortening/truncation, of which the main idea is to allow interference partially in order to reduce the noise boost which can be severe if the channel inversion is used. Once the channel is converted into a poly-diagonal form, the trellis decoding is applied by utilizing the poly-diagonal structure of the underlying channel. As in linear detectors and sphere decoding, poly-diagonalization can also be performed either in ZF sense or in MMSE sense.

Let $\mathbf{B}_L$ be a $N_R \times N_T$ poly-diagonalization matrix of order L such that, for arbitrary diagonal matrices, $\mathbf{D}_l$, $l = 0, \ldots, L-1$, the MIMO channel is effectively poly-diagonalized; i.e.,

$$\mathbf{y}' = \mathbf{B}_L^H \mathbf{y} = \left(\sum_{l=0}^{L-1} \mathbf{D}_l^{(l)} \right) \cdot \mathrm{s} + \mathbf{n}' \tag{9}$$

where the effective channel is represented by a sum of shifted diagonal matrices, i.e., the poly-diagonal form. Each column of $\mathbf{B}_L$, $\mathbf{b}_{L,k}$, can be obtained by first dividing the channel matrix into three terms; the desired signal, $\mathbf{h}_k$, the 'don't cares', $\mathbf{H}_{L,k}$, and the interferences to be nullified or suppressed, $\overline{\mathbf{H}}_{L,k}$. For the poly-diagonalization in the ZF sense (PD-ZF), $\mathbf{b}_{L,k}$ is given by

$$\mathbf{a}_{L,k} = \left(\mathbf{I} - \overline{\mathbf{H}}_{L,k} (\overline{\mathbf{H}}_{L,k}^H \overline{\mathbf{H}}_{L,k})^{-1} \overline{\mathbf{H}}_{L,k}^H \right) \cdot \mathbf{h}_k \tag{10}$$

asymmetric formulation:

$$\mathbf{b}_{L,k} = \left(\mathbf{I} - \overline{\mathbf{H}}_{L,k} (\overline{\mathbf{H}}_{L,k}^H \overline{\mathbf{H}}_{L,k})^{-1} \overline{\mathbf{H}}_{L,k}^H \right) \cdot \mathbf{h}_{k-L+1} \tag{11}$$

where the term in the parenthesis is the projection matrix which projects the desired vector, $\mathbf{h}_k$, onto the null space of $\overline{\mathbf{H}}_{L,k}$ [13]. And, for the poly-diagonalization in the MMSE sense (PD-MM), $\mathbf{b}_{L,k}$ is given by

$$\mathbf{a}_{L,k} = (\overline{\mathbf{H}}_{L,k}\overline{\mathbf{H}}_{L,k}^H + \sigma_n^2\mathbf{I})^{-1} \cdot \mathbf{h}_k \tag{12}$$

asymmetric formulation:

$$\mathbf{b}_{L,k} = (\overline{\mathbf{H}}_{L,k}\overline{\mathbf{H}}_{L,k}^H + \sigma_n^2\mathbf{I})^{-1} \cdot \mathbf{h}_{k-L+1} \tag{13}$$

once the channel is converted into a poly-diagonal form, the trellis decoding is applied for joint detection. The post decoding can be summarized as follows: Let us first define the state vector of the kth trellis stage as $\mathbf{s}_k = \left(s_k, s_{(k-1)_{N_T}}, ..., s_{(k-L+2)_{N_T}}\right)$. For a pair of vectors $\mathbf{x} = (x_0, x_1, \ldots, x_{L-2})$ and $\mathbf{x}' = (x'_0, x'_1, \ldots, x'_{L-2})$, $\mathbf{x}, \mathbf{x}' \in A^{L-1}$, the branch metric is defined as

$$\gamma_k^{(f)}(\mathbf{x}, \mathbf{x}') = \left(\frac{p(\mathbf{s}_k = \mathbf{x})}{p(y'_k)}\right) p(y'_k \mid \mathbf{s}_k = \mathbf{x}, \mathbf{s}_{k-1} = \mathbf{x}') \tag{12}$$

where $p(\mathbf{s}_k = \mathbf{x}) / p(y'_k)$ is a constant for uniform *a priori* probability and the transition probability is given by

$P(y'_k \mid \mathbf{s}_k, \mathbf{s}_{k-1}) = \frac{1}{\sqrt{2\pi}\sigma'_k} \exp\left(-\frac{1}{2\sigma_k'^2}\left|y'_k - \sum_{l=0}^{L-1} a_{kl} s_{(k-l)_{N_T}}\right|^2\right)$ with $a_{kl} = \mathbf{a}_{L,k}^H \mathbf{h}_{(k-l)_{N_T}}$, and $\sigma_k'^2 = \sigma_n^2 \mathbf{a}_{L,k}^H \mathbf{h}_k$.

asymmetric formulation:

$$\gamma_k^{(b)}(\mathbf{x}, \mathbf{x}') = \left(\frac{p(\mathbf{s}_k = \mathbf{x})}{p(y'_k)}\right) p(y'_k \mid \mathbf{s}_k = \mathbf{x}, \mathbf{s}_{k-1} = \mathbf{x}') \tag{13}$$

Where $P(y'_k \mid \mathbf{s}_k, \mathbf{s}_{k-1}) = \frac{1}{\sqrt{2\pi}\sigma''_k} \exp\left(-\frac{1}{2\sigma_k''^2}\left|y'_k - \sum_{l=0}^{L-1} b_{kl} s_{(k-l)_{N_T}}\right|^2\right)$

with $b_{kl} = \mathbf{b}_{L,k}^H \mathbf{h}_{(k-l)_{N_T}}$, and $\sigma_k''^2 = \sigma_n^2 \mathbf{b}_{L,k}^H \mathbf{h}_{k-L+1}$. Using this branch metric, the forward-backward recursion can be effectively implemented in log-domain as follows:

[Initialization]

$\alpha_1(\mathbf{x}) = \beta_{N_T}(\mathbf{x}) = 2^{-\Omega}$

[Recursion]

$$\log \alpha_k(\mathbf{x}) = \max_{\mathbf{x}' \in T_p(\mathbf{x})} \left(\log \gamma_k^{(f)}(\mathbf{x}, \mathbf{x}') + \log \alpha_{k-1}(\mathbf{x}')\right) \quad \text{for } k = 2, 3, \ldots.. \tag{13}$$

$$\log \beta_k(\mathbf{x}) = \max_{\mathbf{x}' \in T_n(\mathbf{x})} \left(\log \gamma_{k+1}^{(b)}(\mathbf{x}', \mathbf{x}) + \log \beta_{k-1}(\mathbf{x}')\right) \quad \text{for } k = N_T \tilde{}\, 1, N_T \tilde{}\, 2, \ldots.. \tag{14}$$

where $T_p(\mathbf{x})$ and $T_n(\mathbf{x})$ are the set of states of the previous and the next trellis stage, respectively, connected to the state vector labeled as $\mathbf{x}$ of the current stage. Note that due to the tail-biting structure of the channel, the recursion can be iterated indefinitely and, indeed, we need more recursions than the number N_T to produce reliable state distribution of edge antennas, i.e., the first and the last. As suggested in [14], however, 2 turns of iterations is enough for the convergence of the state variables.

Once the recursive computation is done, the log *a posteriori* probability estimate is obtained by

$$L(\mathbf{s}_k = \mathbf{x}) = \log \alpha_k(\mathbf{x}) + \log \beta_k(\mathbf{x}) \tag{15}$$

and the LLR for each bit, say the mth, is obtained by

$$L_m = \max_{\mathbf{x} \in A_m^1} L(\mathbf{s}_k = \mathbf{x}) - \max_{\mathbf{x} \in A_m^0} L(\mathbf{s}_k = \mathbf{x}) \tag{16}$$

where $A_m^b \subset A^{L-1}$ denotes the set of data symbols whose mth bit (included in the vector $\mathbf{s}_k$) is equal to b.

4. Simulation Results

4.1. Complexity

The computational complexity of several arithmetic operations can be summarized in Table 1 [17]. A refers to real addition, M refers to real multiplication, A_C refers to complex addition, M_C refers to complex multiplication. In the following, the complexity of the algorithms is given in terms of complex floating point operations (flops). A complex multiplication/division requires 3 flops, and complex addition requires 1 flops.

Table 1 Computational complexity of arithmetic operations

Operation	Inputs	Outputs	Complexity	Flops
Complex multiplication	Two complex	Complex	4M+2A	3.0
Complex by real	Complex and real	Complex	2M	1.0
Square root	Real	Real	M	0.5
Complex power	Complex	Real	2M+A	1.5
Real division	Two real	Real	M	0.5
Complex division	Two complex	Complex	8M+3A	5.5
Complex division	Complex and real	Complex	2M	1.0

The flops of detectors:

$$C_{KLSD\text{-}ZF}(\text{flops}) = 4N_T^2 N_R + \frac{3}{4}N_T^2 - N_T N_R - \frac{3}{4}N_T + \left(4N_T + \frac{3}{2}\right)\sum_{i=1}^{N_T} i \cdot N(\mathbf{s}_i^{N_T}) + \frac{11}{2}N_R N_T K + \frac{3}{2}N_R\Omega + \frac{3}{2}$$

$C_{KLSD\text{-}MM}$(flops)

$$= \frac{4}{3}N_T^3 + 4N_T^2 N_R + \frac{5}{4}N_T^2 - N_T N_R - \frac{13}{12}N_T + \left(4N_T + \frac{3}{2}\right)\sum_{i=1}^{N_T} i \cdot N(\mathbf{s}_i^{N_T}) + \frac{11}{2}N_R N_R K + \frac{3}{2}N_R + \frac{3}{2}$$

$C_{ASY\text{-}PD\text{-}ZF}$(flops)

$$= N_T\left(8N_R N_{N_T-L}^2 + 4N_{N_T-L}^3 - N_R N_{N_T-L} + 4N_R^2 N_{N_T-L} + 8N_R^2 + 2N_R - N_{N_T-L}^2\right) - N_T^2 + 4N_T^2 N_R + 2^{2\cdot\Omega(L-1)}\left(4L+5\right) + 2\cdot N_R \cdot 2\left(\frac{3}{2}2^{2\Omega(L-1)} + \frac{1}{2}2^{\Omega(L-1)} - 1\right) + \frac{1}{2}N_R 2^{\Omega(L-1)} + \frac{1}{2}N_R\Omega$$

$C_{ASY\text{-}PD\text{-}MM}$(flops)

$$= N_T(4N_R^2 N_{N_T-L} + \frac{17}{2}N_R^2 + 4N_R^3 + 2N_R - \frac{1}{2}) - N_T^2 + 2\cdot N_R \cdot 2\left(\frac{3}{2}2^{2\Omega(L-1)} + \frac{1}{2}2^{\Omega(L-1)} - 1\right) + 4N_T^2 N_R + 2^{2\cdot\Omega(L-1)}\left(4L+5\right) + \frac{1}{2}N_R 2^{\Omega(L-1)} + \frac{1}{2}N_R\Omega$$

4.2. Performance

For the performance evaluation, link level simulations have been performed on top of coded MIMO-OFDM in a frequency selective fading channels. Regarding the channel model, each path (between a Tx antenna and a Rx antenna) is assumed to experience uncorrelated frequency selective fading with power profile: [0, -3, -6, -9, -12] (dB) and delay profile: [0, 1, 2, 3, 4] (samples). The power profile was normalized to 1.

The BER performance comparisons of KLSD and ASY-PD for 6×6 antenna configuration, 4QAM modulation and diffident code rate are shown in Figure.1. The tendency in KLSD, where the performance difference between ZF and MMSE preprocessor is obvious for 4QAM and the gap between ZF and MMSE preprocessor will get smaller with the size of candidate for given modulation size [18] and the performances are improved with the variable *K* increased. The Asymmetrical PD shows similar tendency, i.e., the PD in ZF and MMSE shows a distinguishable difference for 4QAM and the performances get better with the variable *L* increased except *L* equal five. This tendency corresponds to the analytical results in [14].

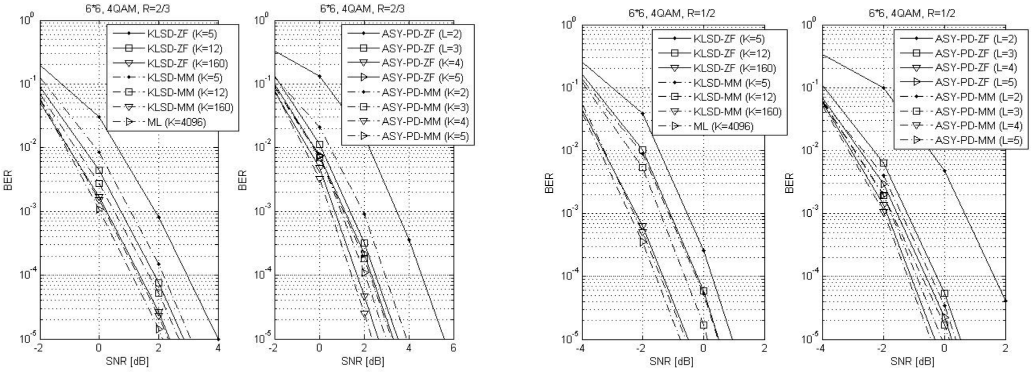

Fig. 1. The BER performance comparisons of KLSD and ASY-PD

4.3. Tradeoff Behavior

Table 2 and Figure.2 demonstrate the tradeoff behavior of the detectors with their variables for 6×6 antenna configuration, 4QAM modulation and diffident code rate. It shows the SNR [dB] when BER is 10^{-4} and the Flops for the KLSD and Asymmtrical PD respectively. The performance of KLSD has an advantage over PD for the code rate is high (i.e., R=2/3) while ASY-PD is better to KLSD for the low code rate (i.e., R=1/2) in the less complexity.

Table 2 Tradeoff Behavior $(6\times6,\ 4\text{QAM})$

		***K*=5**	***K*=12**	***K*=160**	***K*=4096** (ML)
KLSD-ZF	***SNR (dB) (2/3)***	3.0	1.83	1.33	1.0
	SNR (dB) (1/2)	0.2	-0.2	-1.35	-1.5
	Flops	11958	26196	243996	1601052
KLSD-MM	***SNR (dB) (2/3)***	2.2	1.7	1.3	1.0
	SNR (dB) (1/2)	-0.21	-0.6	-1.38	-1.5
	Flops	12262	26500	244300	1601356
		***L*=2**	***L*=3**	***L*=4**	
ASY-PD-ZF	***SNR (dB) (2/3)***	4.6	2.5	1.51	
	SNR (dB) (1/2)	1.7	-0.23	-1.19	
	Flops	10894	20648	239058	
ASY-PD-MM	***SNR (dB) (2/3)***	3.0	2.2	1.35	
	SNR (dB) (1/2)	-0.5	-0.72	-1.28	
	Flops	12199	24299	244059	

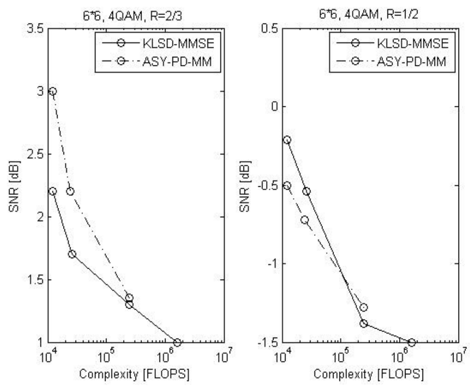

Fig. 2. Tradeoff behavior (6×6, 4QAM)

5. Conclusion

This paper has presented the comparisons of two detector algorithms in MIMO-OFDM systems, i.e, *K*-Best Sphere detectors (KLSD), Asymmetrical Poly-diagonalization in ZF and MMSE senses and tail-biting trellis detectors (ASY-PD) in coded transmissions and frequency selective fading channels. We present how to get the soft-output of both detection algorithms in section 3 and compare the performance and complexity of the detection algorithms in section IV. Judging from the tradeoff behavior, we find the performance of the former has an advantage over the latter for the code rate is high while the latter is superior to the former for the code rate is low in the less complexity. Anyhow, the two algorithms effectively provide a tradeoff between complexity and performance, and the choice of detection scheme can be based further on easiness of hardware implementation and so on.

6. References

[1] L.J. Cimini, "Analysis and simulation of a digital mobile channel using orthogonal frequency division multiplexing," IEEE Trans. Commun, vol.33, no.7, pp.665-675, 1985

[2] G.J. Foschini and M.J. Gans, "On the Limits of Wireless Communications in a Fading Environment When Using Multiple Antennas," *wireless pers.Commun*.,vol.6, no, 3, pp. 311-335,1998

[3] R. Van Nee. A. Van Zelst, and G. Awater, "Maximum Likelihood Decoding in a Space Division Multiplexing System," *Proc. of* VTC 2000, Vol. 1, pp. 6-10 Tokyo, Japan, May 2000

[4] B.M. Hochwald and S.ten Brink, "Achieving Near-Capacity on Multiple-Antenna Channel," *IEEE Trans. On Commun*, Vol.51, No.3, pp.389-399, March 2003

[5] R. Lupas and S. Verdu, "Linear Multiuser Detectors for Synchronous Code Division Multiple-Access Channels," *IEEE Trans. On Info. Theory*, Vol.35, No.1, pp.123-136, 1989

[6] U. Madhow and M.L. Hoaig, "MMSE Interference Suppression for Direct Sequence Spread Spectrum CDMA," *IEEE Trans. on Comm,* Vol.42, No.12, pp.3178-3188, 1994

[7] S.T. Chung, A. Lozano and H.C. Huang , "Approaching Eigenmode BLAST Channel Capacity using V-BLAST with Rate and Power Feedback," *Proc. VTC* 2001 Fall, pp.915-919, Oct 2001

[8] B. Hassibi, " An Efficient Square Root Algorithm for BLAST," in *Proc. IEEE International Conference on Acoustics, Speech, and Signal* Processing (ICASSP'00), Istanbul, Tuekey, June 2000

[9] D. Wubben, R. Boehnke, V. Kuehn, and K. Kammeyer, " MMSE Extension of V-BLAST based on Sorted QR Decomposition," *in Proc. IEEE semiannual Vehicular Technology Conference (VTC2003-Fall),* Orlando, USA, Oct 2003

[10] M. Myllyla, P. Silvola, M. Juntti, J.R. Cavallaro, "Comparison of Two Novel List Sphere Detector Algorithms for MIMO-OFDM Systems," *Proceedings of the IEEE International Symposium on Personal, Indoor, and Mobile Radio Communications*, Helsinki, Finland, pp.12-16, 2006

[11] T.A. Huynh, D.C. Hoang, M.R. Islam and J. kim, " Two-Level-Search Sphere Decoding Algorithm for MIMO Detection," *IEEE International Symposium on Wireless Communication* Systems (ISWCS'08), Reykjavik, Iceland, Oct 2008

[12] K. Higuchi, H. Kawai, H.Taoka, N. Maeda and M. Sawahshi, "Adaptive Selection of Surviving Symbol Replica candidates for Quasi-Maximum Likelihood Detection Using M-Alorithm with QR-Decomposition for OFDM MIMO Multiplexing," *IEICE Transactions on Communications,* Vol.e92-b, 2009

[13] S. Yoon and S. Lee, "A Detection Algorithm for Multi-input Multi-Output (MIMO) Transmission using Poly-Diagonalization and Trellis Decoding," *IEEE J. on Sel. Areas Commun*, Vol.26, No.6, pp.993-1002, Aug 2008

[14] S. Yoon, "Asymmetrically optimized poly-diagonalisation for low complexity MIMO detection," Electronics Letters, Vol.46, No.17, Aug 2010

[15] S. Schwandter, P. Fertl, C. Novak and G. Matz. "Log-likelihood ratio clipping in MIMO-BICM systems: information grometric analysis and impact on system capacity," *Proc. IEEE ICASSP,* pp.2433-2436, Taipei, Taiwan, 2009

[16] Y.C. de Jong and T. Willink, "Iterative tree search detection for MIMO wireless systems," *IEEE Trans. On Commun*, Vol. 53, No.6, June, 2005

[17] Auda M. Elshokry, *Complexity and Performance Evaluation of Detection Schemes,* Islamic University, 2010

[18] Ernesto Zimmermann, *complexity aspects in Near-capacity MIMO detection-decoding*, Dresden Techn. Univ, 2007